The functional importance of human foot muscles for bipedal locomotion

Dominic James Farris[a,b,1], Luke A. Kelly[b], Andrew G. Cresswell[b], and Glen A. Lichtwark[b]

[a]Sport & Health Sciences, College of Life & Environmental Sciences, University of Exeter, St Luke's Campus, EX1 2LU Exeter, United Kingdom; and [b]School of Human Movement & Nutrition Sciences, The University of Queensland, Brisbane, QLD 4072, Australia

Edited by Bruce Latimer, Case Western Reserve University, Cleveland, OH, and accepted by Editorial Board Member C. O. Lovejoy December 13, 2018 (received for review July 25, 2018)

Human feet have evolved to facilitate bipedal locomotion, losing an opposable digit that grasped branches in favor of a longitudinal arch (LA) that stiffens the foot and aids bipedal gait. Passive elastic structures are credited with supporting the LA, but recent evidence suggests that plantar intrinsic muscles (PIMs) within the foot actively contribute to foot stiffness. To test the functional significance of the PIMs, we compared foot and lower limb mechanics with and without a tibial nerve block that prevented contraction of these muscles. Comparisons were made during controlled limb loading, walking, and running in healthy humans. An inability to activate the PIMs caused slightly greater compression of the LA when controlled loads were applied to the lower limb by a linear actuator. However, when greater loads were experienced during ground contact in walking and running, the stiffness of the LA was not altered by the block, indicating that the PIMs' contribution to LA stiffness is minimal, probably because of their small size. With the PIMs blocked, the distal joints of the foot could not be stiffened sufficiently to provide normal push-off against the ground during late stance. This led to an increase in stride rate and compensatory power generated by the hip musculature, but no increase in the metabolic cost of transport. The results reveal that the PIMs have a minimal effect on the stiffness of the LA when absorbing high loads, but help stiffen the distal foot to aid push-off against the ground when walking or running bipedally.

gait | intrinsic foot muscles | biomechanics | longitudinal arch | bipedal locomotion

The pronounced long arch (LA) of the human foot is a key structural feature that distinguishes our feet from those of other primates and our common ancestors (1, 2). Its evolution can be traced from the earliest hominin pedal fossil remains of *Ardipithecus ramidus* (ca. 4.4 million years old), through australopithecine specimens (ca. 3–4 million years old), to the genus Homo (3). *A. ramidus* was observed to have a highly abducted and opposable hallux (4) that progressively became fully adducted (Fig. 1) by the emergence of *Homo habilis* and *Homo erectus*, ∼2.5 million years later (5, 6). Through this hallucal adduction and realignment of midfoot bones, the distinct LA now prominent in the feet of humans became apparent (Fig. 1). This intricate restructuring of bones within the foot is thought to have been driven by selection for bipedalism over arboreal locomotion (3), with the latter requiring an opposable hallux for grasping branches. In humans, the LA stiffens the foot, providing leverage for applying propulsive forces to the ground, and is considered advantageous for performing bipedal walking and running (2, 7).

Despite the apparent benefits of a stiff LA for bipedalism, primates are capable of bipedal gait, and the LA of humans is known to exhibit elastic mechanics to absorb and return energy during contact with the ground (8). In fact, this spring-like function provides an important energetic saving for running humans (8), and is considered a further advantage of the LA for bipedalism. Historically, much credit for the elasticity of the LA has been granted to the plantar aponeurosis, a ligamentous structure spanning the arch from the heel to the underside of the toes, wrapping under the metatarsal-phalangeal (MTP) joints that allow the toes to rotate (Fig. 1). The same structure has been vaunted as responsible for stiffening the foot via the windlass mechanism (9). This mechanism proposes that winding of the plantar aponeurosis around the metatarsal heads during late stance raises the LA, and passively stiffens the foot for propulsion (Fig. 1). As such, the plantar aponeurosis has often been considered the most important soft tissue in supporting the LA.

However, growing evidence suggests that the LA is also supported by the plantar intrinsic muscles of the foot (PIMs), a group of muscles situated within the foot below the LA (10–13). Several of the PIMs span the LA in parallel with the plantar aponeurosis (Fig. 1) and are active during contact of the foot with the ground in walking and running (10, 13). Experiments electrically stimulating the PIMs (11) and anesthetically blocking PIM contraction (14) have shown that these muscles influence the mechanical function of the LA when humans are statically bearing weight through their feet. Furthermore, the degree to which these muscles are activated is adjusted in response to varied mechanical loads placed on the foot (13, 15), and anthropological data have linked the size of PIMs to the degree of loading experienced by the foot in everyday life (16). Therefore, the current body of evidence suggests indirectly that the PIMs are significant in stiffening the human foot and supporting its LA. Thus, the PIMs may have a fundamentally important role in the function of the human foot and our evolved specialism for bipedalism. However, to date, there is no direct experimental

Significance

Human feet have evolved uniquely among primates, losing an opposable first digit in favor of a pronounced arch to enhance our ability to walk and run with an upright posture. Recent work suggests that muscles within our feet are key to how the foot functions during bipedal walking and running. Here we show direct evidence for the significance of these foot muscles in supporting the mechanical performance of the human foot. Contrary to expectations, the intrinsic foot muscles contribute minimally to supporting the arch of the foot during walking and running. However, these muscles do influence our ability to produce forward propulsion from one stride into the next, highlighting their role in bipedal locomotion.

Author contributions: D.J.F., L.A.K., A.G.C., and G.A.L. designed research; D.J.F. and L.A.K. performed research; D.J.F., L.A.K., and G.A.L. analyzed data; and D.J.F., L.A.K., A.G.C., and G.A.L. wrote the paper.

The authors declare no conflict of interest.

This article is a PNAS Direct Submission. B.L. is a guest editor invited by the Editorial Board.

Data deposition: Data related to this paper have been deposited at https://doi.org/10.14264/uql.2019.3.

[1]To whom correspondence should be addressed. Email: d.farris@exeter.ac.uk.

This article contains supporting information online at www.pnas.org/lookup/suppl/doi:10.1073/pnas.1812820116/-/DCSupplemental.

Published online January 17, 2019.

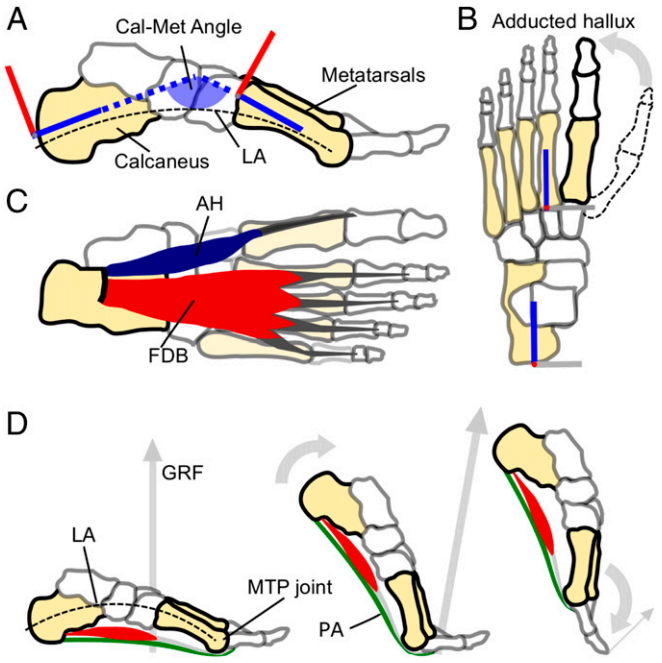

Fig. 1. Salient features of the human foot, and the windlass mechanism in action. (*A*) A medial view of the human foot bones highlighting the pronounced longitudinal arch (LA, dashed line) and a schematic illustration of the Cal-Met angle that we used as a measure of dynamic arch compression (the angle formed between the calcaneus and metatarsal segments of the foot model, as defined in ref. 43). (*B*) Superior view of the human foot bones with a depiction of how the human hallux (bold outline) is greatly adducted from the opposable hallux found in fossil remains of our hominin ancestors (e.g., dashed outline). (*C*) A plantar view of the human foot showing the largest superficial PIMs that span the LA and MTP joints: Abductor hallucis (AH) and FDB. The PIMs also include abductor digiti minimi, quadratus plantae, flexor hallucis brevis, the lumbricals, and adductor hallucis (17), which have not been included here for clarity. (*D*) Depicts the windlass mechanism in action from mid to late stance in human walking. From left to right, the foot rotates about the MTP joints, tensioning the plantar aponeurosis (PA) and raising the LA (decreasing the Cal-Met angle) before the toes are plantar flexed as the PA recoils just before toe-off.

evidence to support the importance of the PIMs for foot function during human walking and running.

Therefore, this experiment aimed to test the importance of the PIMs for stiffening the human foot, for providing LA support, and for generating propulsion during human walking and running. To do so, we used a posterior tibial nerve block to prevent activation of the PIMs in two experiments. In the first, controlled loading of the lower leg was applied via a linear actuator with and without a tibial nerve block. We hypothesized that the LA of the foot would compress more in response to applied loads when the nerve block was in place, demonstrating the importance of the PIMs in providing active support to the LA under load. In the second experiment, participants walked and ran on a treadmill with and without a tibial nerve block to both feet. This experiment aimed to determine the importance of the intrinsic muscles in supporting the LA during weight acceptance, and in stiffening the foot to act as a lever against the ground in late stance. We examined lower limb and foot mechanics and whole-body metabolic cost of transport (CoT). We hypothesized that an inability to activate the PIMs during walking and running would inhibit stiffening of the LA to resist rising ground contact forces in early stance, inhibit the generation of push-off against the ground during late stance, and lead to increased stride frequency and hip joint work to compensate for the lack of push off (17), resulting in an increased rate of metabolic energy consumption (less efficient gait).

Results

The Nerve Block. Measurement of the peak-to-peak M-wave response of the flexor digitorum brevis (FDB; Fig. 1*C*) muscle to percutaneous electrical stimulation of the tibial nerve confirmed the effectiveness of the nerve block in dramatically reducing plantar intrinsic muscle activation for both experiments (e.g., Fig. 2*A*). The FDB peak-to-peak M-wave magnitude was reduced, on average by 90 ± 9%.

Experiment 1: Controlled Loading. Compression of the LA was measured by changes in the Cal-Met angle formed between the calcaneus and metatarsal segments (illustrated in Fig. 1*A*). Peak vertical ground reaction force (vGRF) during loading cycles was varied between 0.5 and 2.5 body weights and produced proportional changes in the Cal-Met angle (Fig. 2*C*). There was a significant effect of the nerve block on LA deformation, with the changes in Cal-Met angle being greater for equivalent peak forces in the nerve block condition, although only by modest magnitudes (<1° difference in group means; Fig. 2*C*).

Experiment 2: Walking and Running. Despite the inability to activate the intrinsic foot muscles, the nerve block produced no change in the LA's response to the initial loading of the midfoot, as measured by the increase in the Cal-Met angle in response to the moment generated about the midfoot during early-mid stance

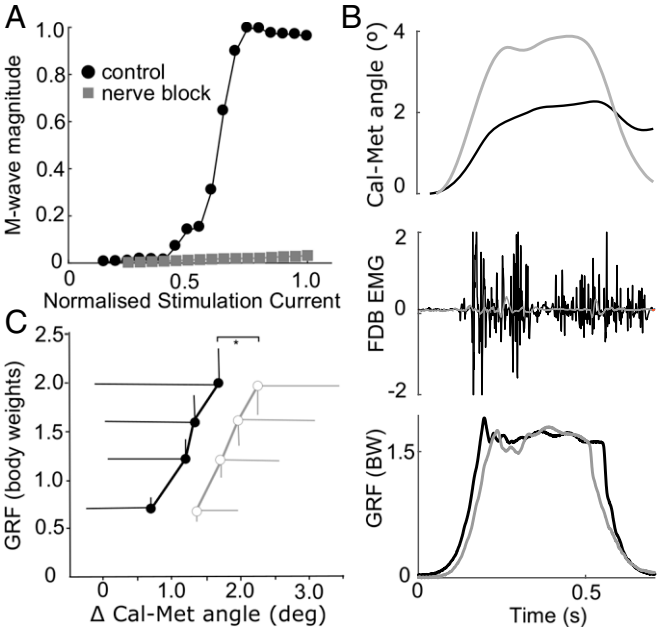

Fig. 2. Data for experiment 1. (*A*) The tibial nerve block dramatically reduced the compound M-wave response of FDB by, on average, 90%. An example participant's M-wave recruitment curve plots the normalized stimulation current applied to the tibial nerve (relative to maximum) vs. the M-wave peak-to-peak amplitude (relative to maximum). No M-wave response was recorded in the nerve block condition (gray), indicating a successful motor block. (*B*) Exemplar data ($n = 1$, single load cycle) for a 1.5 body-weight static loading cycle showing vGRF (*Bottom*), FDB raw electromyographic activity (EMG) (*Middle*), and long arch deformation measured by the change in angle formed between the calcaneus and metatarsal segments (Cal-Met angle; *Top*). Gray lines, nerve block; black lines, control condition. (*C*) The deformation of the long arch as measured by the peak change in the Cal-Met angle was greater under equivalent loading in the nerve block condition ($n = 12$; MLRT $^*P < 0.05$). Data are group mean (±SD) peak vGRF vs. change in Cal-Met angle, during loading cycles (black/filled, control; gray/open, nerve block).

(Fig. 3*H*). However, there was a significant [maximum likelihood ratio test (MLRT), $P = 0.026$] effect of the nerve block of reducing the angular impulse generated by the midfoot moment during recoil of the arch (walking: 6.4 ± 2.2 N·m·s vs. 5.2 ± 1.5 N·m·s; slow: 9.4 ± 2.4 N·m·s vs. 8.1 ± 2.3 N·m·s; faster: 9.4 ± 2.5 N·m·s vs. 8.7 ± 2.6 N·m·s). During late stance, the nerve block induced a reduction in stiffness of the MTP joint as vGRF fell and the toes dorsiflexed (Fig. 3 *A, C, E*, and *G*). This reduction in MTP joint stiffness was linked more to a reduction in MTP joint moment than to changes in MTP dorsiflexion range of motion (Fig. 3 *A, C*, and *E*).

The nerve block significantly affected the ability of participants to generate positive power and work through the foot and ankle during late stance. It can be seen in Fig. 4 that foot positive power production was less in the nerve block condition, resulting in significantly less positive work at the foot in walking (3.3 ± 2 J/stride vs. 5.1 ± 2 J/stride, $P = 0.004$) and both running (slow: 9.1 ± 6 J/stride vs. 13.6 ± 6 J/stride; $P = 0.002$; faster: 9.8 ± 7 J/stride vs. 13.7 ± 7 J/stride; $P = 0.007$; Fig. 5) conditions. Furthermore, Fig. 5 shows that a decrease in positive ankle joint work was observed for both running speeds under the nerve block condition (slow: 58.6 ± 19 J/stride vs. 67.0 ± 20 J/stride, $P = 0.008$; faster: 66.1 ± 22 J/stride vs. 71.3 ± 20 J/stride, $P = 0.04$). From Fig. 4 *A* and *C*, this appears to coincide with marginally lower ankle power production through late stance (after peak positive power) for the nerve block condition. The analysis of the linear mixed model showed that the nerve block also resulted in participants generating greater positive work about the hip (MLRT: $P = 0.004$; Fig. 5). Post hoc tests showed this difference was significant for walking and faster running, but not slow running (walking: 30.2 ± 8 J/stride vs. 24.7 ± 7 J/stride, $P = 0.002$; slow: 68.7 ± 24 J/stride vs. 74.9 ± 20 J/stride, $P = 0.1$; faster: 90.3 ± 21 J/stride vs. 83.1 ± 27 J/stride, $P = 0.045$).

Comparisons of data, including all speeds, showed that the propulsive impulse generated through anterior directed ground reaction force significantly decreased when the nerve block was in place (MLRT: $P < 0.001$). Comparisons within speeds further confirmed that the nerve block reduced propulsive impulse during walking and running (walking: 15.4 ± 4 N·s vs. 17.7 ± 4.2 N·s, $P = 0.003$; slow: 9.9 ± 2.5 N·s vs. 11.5 ± 2.6 N·s, $P = 0.002$; faster: 9.7 ± 2.6 N·s vs. 11.5 ± 2.6 N·s, $P = 0.002$).

A final notable effect of the nerve block was that it caused an increase in stride frequency (walking: 1.03 ± 0.09 Hz vs. 0.98 ± 0.07 Hz, $P = 0.01$; slow: 1.52 ± 0.09 Hz vs. 1.45 ± 0.08 Hz, $P < 0.001$; faster: 1.59 ± 0.10 Hz vs. 1.49 ± 0.10 Hz, $P = 0.007$). However, there was no change in the metabolic CoT for walking or running with the nerve block (walking: 0.24 ± 0.03 $J{\cdot}N^{-1}{\cdot}m^{-1}$ vs. 0.24 ± 0.03 $J{\cdot}N^{-1}{\cdot}m^{-1}$, *t* test $P = 0.44$; slow: 0.41 ± 0.05 $J{\cdot}N^{-1}{\cdot}m^{-1}$ vs. 0.41 ± 0.03 $J{\cdot}N^{-1}{\cdot}m^{-1}$, *t* test $P = 0.26$).

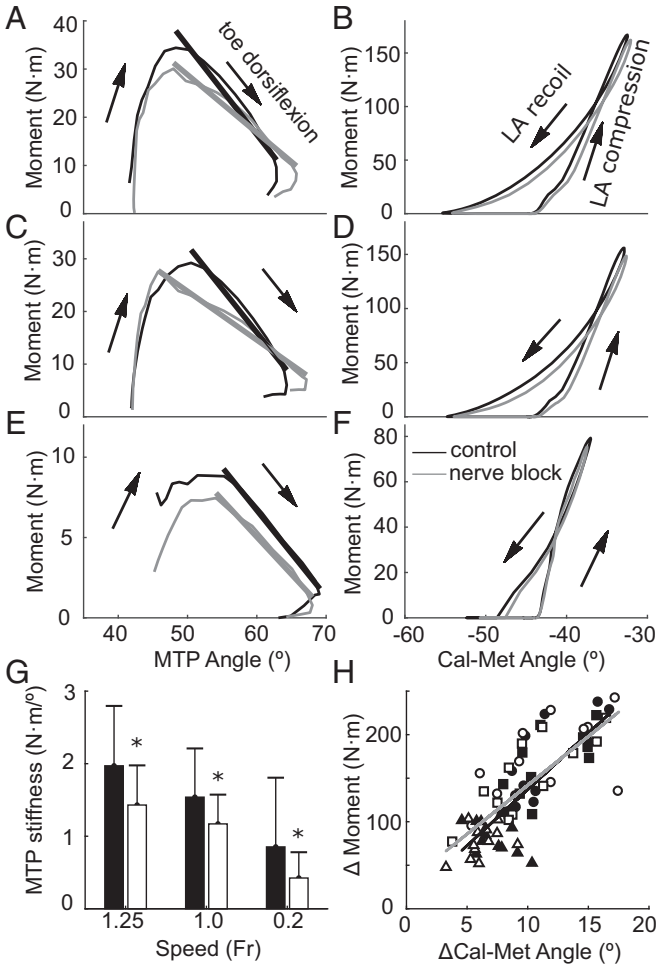

Fig. 3. The stiffness of the MTP joint during late stance was greater in the control condition than in the nerve block condition, but there was no change in stiffness of the long arch. *A*, *C*, and *E* plot the MTP angle against the MTP moment for running (*A*: Fr = 1.25; *C*: Fr = 1.0) and walking (*E*, Fr = 0.2), and each has a linear fit to illustrate the stiffness of the joint late in stance (black, control; gray, nerve block). *G* shows a bar graph of the mean (±SD) stiffness values (slope) from the linear fits in *A*, *C*, and *E* for each speed and highlighting a significant effect of the nerve block (N = 12; $P < 0.05$) with asterisks. *B*, *D*, and *F* plot the Cal-Met angle vs. the midfoot moment to approximate the stiffness of the long arch (control, black; nerve block, gray). There was no effect of the nerve block on long arch stiffness during loading. Across all speeds, the peak deformation of the long arch (ΔCal-Met angle) increased with increasing midfoot moment (*H*), but linear fits to the data show that this relationship was unaffected by the nerve block (gray/open symbols, nerve block; black/filled symbols, control; triangles, walking; squares, slow running; circles, faster running).

Discussion

The long arch of the human foot is highly evolved to both suit elastic absorption of energy and provide a stiff foot to push against the ground. Both are key adaptations for obligate bipedal gait. Our data show that the elastic absorption of energy by the LA is only minimally supported by contraction from the plantar intrinsic foot muscles. However, without active contraction of these muscles, stiffening of the forefoot during push-off against the ground is impaired, and our ability to generate propulsive power is affected. These findings significantly modify our current understanding of the functional significance of the PIMs and human foot mechanics during bipedal gait.

The unique structure of the LA allows the foot to deform under load, stretching the plantar aponeurosis and PIMs that span its length, and storing energy in these tissues. The arch is supported in resisting this deformation by elastic tensioning of the plantar aponeurosis (8), and was thought to gain significant additional support from active contraction of the PIMs (13). Initial results from Experiment 1 showed that eliminating contraction of the PIMs did inhibit the ability of the LA to resist an applied load, reducing the change in Cal-Met angle by 1° (Fig. 2*C*). However, the small deformations of the LA in Experiment 1 (2–3° change in Cal-Met angle; Fig. 2*C*) highlighted that the load borne by the LA was far less than during walking and running, where the Cal-Met angle changed by ∼20° (Experiment 2). For walking and running, we observed no effect of the nerve block on the deformation of the LA, its peak value, the peak midfoot moment, or midfoot stiffness (Fig. 3 *B, D*, and *F*). Therefore, we believe that during gait, the contribution of the PIMs to LA support during weight acceptance is minimal. This conclusion is at odds with our group's previous inferences based on electromyographic activity recordings from the PIMs. However, this can be reconciled by considering the force potential of the PIMs. From

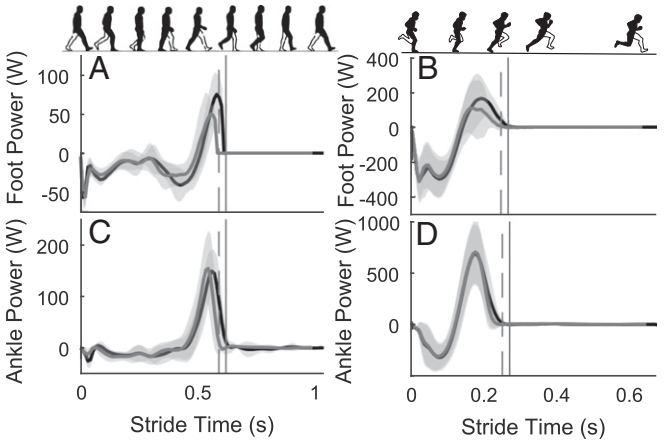

Fig. 4. Positive power produced by the foot and ankle in late stance was reduced by the nerve block. Group mean (±SD) time series power data for the foot (*A* and *B*) and ankle joint (*C* and *D*). The left column is data from walking (Fr = 0.2) and is scaled differently to the right column, which is faster running (Fr = 1.25). Across all speeds, the distal foot produced less positive power in late stance in the nerve block condition (gray lines) compared with the control condition (black lines). Ankle positive power in late stance dropped earlier across all speeds for the nerve block condition, and this was linked with reduced stance and stride times when the nerve block was applied. Data are plotted from foot–ground contact to ipsilateral foot–ground contact, and the vertical lines represent the end of the stance phase for control (solid) and nerve block (dashed) conditions, respectively. Power data for all leg joints, in all conditions are provided in *SI Appendix* (*SI Appendix*, Fig. S1).

cadaver data (18), the combined physiological cross-sectional area of FDB, quadratus plantae, and abductor hallucis is 15 cm^2. Multiplied by a specific tension of 25 $N{\cdot}cm^2$ (19–21), the combined maximum isometric force for the main PIMs is 375 N. Assuming a generous moment arm of these muscles about the midfoot (navicular) of 4 cm, the maximum moment the PIMs could produce about the midfoot is 15 N·m. This is ∼10% of the maximum midfoot moment during running (Fig. 3*F*) and supports the notion that these muscles can only contribute minimally to resisting LA deformation during the midstance phase of gait, when the LA is subjected to the greatest load.

That these muscles do not provide significant support to the LA was against our hypothesis. It suggests that the supporting soft tissues of the LA have evolved alongside the bony structures to bear the majority of external loading in passive elements such as the plantar aponeurosis, as supposed by Ker et al. (8). The plantar aponeurosis (and other pedal ligaments) can elastically store and return energy without directly consuming metabolic energy, and are less massive than a muscle producing similar forces. Thus, reliance on passive tissues to bear loads could help minimize energetically costly distal limb mass. Retrospective studies have shown that individuals who habitually wear minimal footwear have a lower incidence of pes planus (flat feet) (22), have stiffer LAs (16), and have larger PIMs (16). From such evidence, it could be induced that larger, stronger PIMs are mechanistically linked to the loading of feet in everyday life, and that working them in early life could protect against the development of the pes planus condition. Although we do not know whether the relative contributions to LA support are similar or not in children, our findings suggest that the elastic properties of the plantar aponeurosis (stiffness or resting length) would be more influential in supporting the development of a higher, stiffer LA.

Although the PIMs do not contribute much to LA support in midstance, our findings did show that the PIMs are important in stiffening the forefoot during late stance, when the foot is being used as a rigid lever for push-off, a theory first purported by Mann and Inman (10). We have shown that removing the ability to activate the PIMs reduces the positive mechanical work done at the foot and ankle during push-off because of an earlier decline in power output in late stance (Fig. 4). Furthermore, the propulsive impulse that participants were able to generate about the midfoot and on the ground was reduced by the nerve block. This all occurred concurrently with a reduced ability to generate moments to stiffen the MTP joint (Fig. 3 *A*, *C*, and *E*).

The reduction in moments about the MTP joint with the nerve block are in line with our estimates of what the PIMs are capable of contributing. We approximated the moment arm of PIMs about the MTP joint to be 1.5 cm (23) and calculated a potential moment contribution of 6 N·m about the MTP joint (using the same muscle parameters as earlier). Although a small moment, this is approximately half the peak MTP joint moment during walking and 20% of the peak in running (Fig. 3 *A*, *C*, and *E*). It is also comparable in magnitude to the drop in MTP moment observed with the nerve block (Fig. 3 *A*, *C*, and *E*), and it is reasonable to state that the PIMs have a significant influence on MTP joint mechanics. Activation of the PIMs in late stance is required to generate sufficient impedance about the MTP joint for an effective push-off through propulsive impulses and ankle joint work. Thus, the role of the foot as a rigid lever in late stance is supported by active muscular contributions. Previously, much of the credit for the foot's rigidity in late stance has been attributed to the windlass mechanism, first observed by Hicks (9), and since considered to occur in gait by dorsiflexion of the toes in late stance tensioning the plantar aponeurosis and stiffening the foot. Our data suggest that this mechanism is insufficient by itself and requires an active force contribution from the PIMs. The PIMs' contribution is fundamentally different from the windlass mechanism, because PIMs that span the LA and MTP joints (e.g., abductor hallucis and FDB) are either isometric or shortening during late stance when propulsion is generated (13). This is because the effect of shortening of the LA exceeds the effect of toe dorsiflexion on PIM length. Therefore, the PIMs are not being tensioned by winding of the toes, but are actively generating tension isometrically, or while shortening, to stiffen the MTP joint.

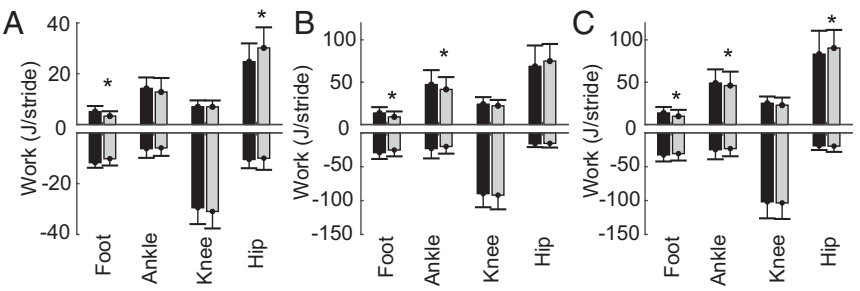

Fig. 5. The nerve block resulted in reduced positive work done at the foot and ankle during walking and running, but increased positive work done at the hip. Group mean (±SD, $n = 12$) positive and negative work done per stride at the foot, ankle, knee, and hip for the control (black) and nerve block (gray) conditions. Data are for walking (*A*), slower running (*B*), and faster running (*C*). Significant effects of the block on a work value were found first by comparison of linear mixed models with and without nerve block as a factor, via the likelihood ratio test (likelihood ratio test: positive distal foot work, $P = 0.0004$; positive ankle work, $P = 0.01$; positive hip work, $P = 0.004$). When the likelihood ratio test was significant, post hoc *t* tests were used within each speed and a Bonferroni correction applied to account for multiple comparisons ($P < 0.05$ was considered significant, indicated by *).

The fact that MTP joint stiffness is actively regulated is of great interest from an evolutionary standpoint, and may have implications for prosthetic design. The MTP joints of the first two rays of the foot permit rotation about a transverse axis (perpendicular to the direction of motion), but the axis of the lateral three MTP joints is more obliquely oriented (24). Rotation of the foot about the transverse axis is considered key for a forceful push-off because it is thought to more effectively engage the windlass mechanism (7). Interestingly, stiffening the first MTP joint could be linked to force production by abductor hallucis, the largest of the PIMs (18). This muscle is also one that was observed to be larger in habitually minimally shod individuals (16). Perhaps humans' uniquely adducted hallux has facilitated the use of the largest intrinsic foot muscle in stiffening the forefoot for effective push-off, in synergy with the windlass mechanism and LA. From another perspective, our findings support the notion that active regulation of an MTP joint stiffness may be necessary in bio-inspired foot prosthetics. A recent experiment adjusting a foot prosthetic has shown that work done on the body center of mass during push off is highly sensitive to the stiffness of the prosthetic's MTP joint (25). This finding also lends support to our results regarding the cascade of mechanical changes that were initiated by the impaired push-off with the nerve block.

The importance of generating propulsive impulses and ankle joint work for push-off in late stance has been well established (17, 26), with the foot performing a critical role (27–30). Without effective push-off during walking, energy is lost in transition between steps and must be compensated for by elevated hip muscle work (17). In agreement with this, the impaired push-off in the nerve block condition led to a compensatory increase in hip joint positive work in late stance and early swing phases of walking and running (Fig. 5 and *SI Appendix*, Fig. S1), along with an elevated stride frequency. All the changes to gait mechanics discussed here would be expected to increase the metabolic CoT (26, 31–35), but we observed no change in the metabolic CoT for walking or running. An explanation for this may be that the shift in stride frequency induced by the nerve block was insufficient to significantly increase the CoT. The relationship between CoT and stride frequency is U-shaped, with preferred stride rate close to the metabolic CoT minimum (26, 31–33). The region around the minimum has a shallow curvature, and one would have to substantially perturb the stride rate of an individual to produce a measurable increase in metabolic CoT. The nerve block resulted in modest increases in stride frequency of 5–6%, and a comparison with existing data (33, 36) suggests that a 5–6% increase in stride frequency above preferred would not notably elevate metabolic CoT. Therefore, although removing PIMs activation significantly affected push-off mechanics, this did not measurably elevate the energetic costs of locomotion.

It should be noted that the nerve block also affects sensory feedback from the plantar surface of the foot, resulting in altered sensation during walking and running. Although it cannot be shown from the present data, studies separating the effect of impaired cutaneous plantar feedback from those of a motor block have shown no effect of impaired cutaneous feedback on gait mechanics (37, 38) or standing balance (39). As such, we believe it is unlikely that the results in the present study were related to altered sensory feedback. It is conceivable that some missing active force contribution of the PIMs to LA support could have been compensated for by increased activation of extrinsic foot muscles, or by passive tension developed via lengthening of the PIMs. The PIMs supporting the LA are mostly short-fibered pennate muscles. An advantage of a pennate structure is that rotation of fibers can accommodate whole muscle length change, rather than fiber lengthening itself (40). Furthermore, the fibers would also have to be stretched well beyond their resting lengths to generate any significant passive tension that could rival their normal active contribution. Therefore, we believe compensation via passive tension was unlikely. It is also conceivable that extrinsic foot muscles (e.g., tibialis posterior, tibialis anterior, and the peroneals) could provide some support to the LA, and potentially might have compensated for the intrinsic muscles in the nerve block condition. However, the anatomical path of the tendons of the extrinsic foot muscles suit them more to providing support in the frontal plane of the foot. Furthermore, their small moment arms about the LA hinders their potential to generate supporting moments. It is therefore doubtful that the extrinsic foot muscles could compensate, but this requires further investigation. The study might have been improved by inclusion of a faster running speed condition. At faster speeds, the PIMs are more active for arch support (13), and therefore a greater effect of the block might have been observed. However, as a result of a limited duration of the nerve block and initial concerns that participants would not complete a faster running speed safely, we were unable to add a faster running condition. Our calculations of maximal force contribution suggest, however, that faster running speeds are unlikely to make a significant difference.

In conclusion, we have shown that the PIMs actively contribute to stiffening of the MTP joint in late stance during walking and running, to assist propulsive push-off, and that the windlass mechanism cannot support this function without them. However, the same muscles are not significant contributors to supporting the long arch of the foot during the weight acceptance phase of gait, and this function must be largely attributed to elastic structures such as the plantar aponeurosis and ligaments within the arch. The human foot evolved over several millennia to have a stiff long arch, an adducted hallux, and short toes that significantly aid our bipedal gaits by forming a stiff lever. The plantar intrinsic foot muscles actively assist this function.

Methods

Two separate experiments were approved by the Bellberry Human Research Ethics Committee for the University of Queensland. Except for the protocols, data collection and analysis techniques were similar and are only described once here. Experiment 1 included 12 participants (eight men, four women; mean ± SD age = 28 ± 5 y; mass = 72 ± 11 kg), as did experiment 2 (nine men, three women; mean ± SD age = 30 ± 6 y; mass = 77 ± 12 kg), all of whom provided written informed consent. Both experiments compared a nerve block condition with a control condition. For the nerve block, an anesthetic block of the tibial nerve was applied at the ankles to prevent contraction of the PIMs (details in *SI Appendix*). The block was confirmed by recording intramuscular fine-wire electromyography signals from FDB (*SI Appendix*) during electrical stimulation of the tibial nerve (Fig. 2). In the control condition, no nerve block was applied.

Protocols. In experiment 1, participants were seated with their knee flexed and one foot on a force platform (AMTI). A custom-built linear motor (LinMot) applied controlled vertical forces to the thigh just proximal to the knee, equivalent to 0.5, 1.0, 1.5, and 2.0 body weights, to statically load the leg (a detailed schematic is presented in *SI Appendix*, Fig. S2). Sets of five cycles at each load were applied in a random order. Participants were instructed to bear the load in a manner that felt most natural to do so. All loading conditions were completed for the nerve block and control conditions. In experiment 2, each participant walked at one speed [Froude number (Fr) = 0.25] and ran at two speeds (Fr = 1.00, Fr = 1.25) on an instrumented treadmill (AMTI Tandem, AMTI). For collection of mechanical data, participants walked or ran for 60 s, and a 15-s trial was collected toward the end of the 60-s period. Metabolic data were recorded during 5 min continuous trials, but only for the walking and slower running conditions. Rates of oxygen consumption and carbon dioxide production were measured during trials with a portable spirometry system (MetaMax 3B; Cortex), and the equations of Brockway (41) were used to calculate the metabolic CoT ($J \cdot kg^{-1} \cdot m^{-1}$) for walking and running in the control and nerve block conditions.

Biomechanical Measurements. 3D motion capture data were recorded with an opto-electronic system (Qualysis). Reflective markers were attached to the pelvis, right leg, and right foot of participants in accordance with the Istituto Ortopedico Rizzoli (IOR) gait model (42) and IOR foot model (43). Using marker positions from a static trial, a rigid body model as defined in refs. 42 and 43 of pelvis, thigh, shank, calcaneus, midfoot, metatarsal, and hallux segments was built and scaled for each participant in Visual 3D software (C-Motion). The same

software was used to model the motion of the segments in walking and running trials. As a measure of the dynamic posture of the LA of the foot, we computed the orientation of the metatarsal segment in the calcaneus reference frame and extracted the Euler angle about the mediolateral axis of the calcaneus (Cal-Met angle; Fig. 1). A positive change in this angle (Cal-Met) represents dorsiflexion of the metatarsals relative to the calcaneus, compression of the LA, and stretch of the plantar aponeurosis and PIMs. The angle of the MTP joint was calculated as the orientation of the hallux segment relative to the metatarsal segment. In accordance with recent recommendations (29), ankle angles were computed as the orientation of the calcaneus with respect to the shank segment. Knee and hip angles were the orientation of the shank and thigh relative to the thigh and pelvis segments, respectively. Joint moments were computed in Visual 3D, using inverse dynamics analysis, with the moment about the midfoot segment only calculated once the center of pressure had progressed anterior to the proximal end of the midfoot. Midfoot moment was considered an estimate of loading on the LA. MTP joint moments were only calculated once the center of pressure was anterior to the distal end of the metatarsal segment. Joint powers (hip, knee, and ankle) were calculated as the dot product of joint moments and velocities. Foot power was calculated as per Takahashi et al. (28) and represents the power resulting from the 6° of freedom movement between the calcaneus and the ground, providing an estimate of combined power from all structures within the foot distal to the calcaneus (29), including structures of the LA. Work values for the foot and other joints are reported as Joules/stride and represent the time integral of either all periods of positive power (positive work) or all periods of negative power (negative work), for that joint over a stride.

Data Analysis for Experiment 1. A linear mixed model was fitted using the *fitlme* function in Matlab (The Mathworks) with change in Cal-Met angle as the dependent variable, fixed effects for nerve block (control or nerve block), integrated FDB electromyographic activity and peak GRF (in body weights), and random effects on slope and intercept for participant. To test for an effect of nerve block on LA compression, a second model was fitted without nerve block as a factor and the two models were compared with the MLRT via Matlab's inbuilt *compare* function. A P value for the MLRT of <0.05 was taken to show a significant effect of the nerve block.

Data Analysis for Experiment 2. Mechanical data were collected over 15-s trials and separated into individual strides (ground contact to ipsilateral ground contact) based on the vertical GRF. Time-series data for each stride were normalized to 101 points and averaged for each participant, and then the group. All data presented (time series and other outcome variables) are group means and SDs unless otherwise stated. To test for an effect of the nerve block on each outcome variable, we again used linear mixed modeling and the MLRT. The model included fixed effects for speed (Fr = 0.25, 1.0, 1.25), nerve block (control or blocked), gait (walk or run), and random effects of participant on slope and intercept. Nerve block was then removed from the model and the two models compared as in Experiment 1. A P value for the MLRT of less than 0.05 was taken to show a significant effect of the nerve block. In Experiment 2, to test the effect of the nerve block within each speed, a paired t test with a Bonferroni correction was used as a post hoc test ($P < 0.05$ as significant). When testing for an effect of nerve block on the Cal-Met angle change, the change in midfoot moment was included as an additional fixed effect.

Data Deposition. Data related to this paper have been deposited at https://doi.org/10.14264/uql.2019.3 (44).

ACKNOWLEDGMENTS. This work was supported by Australian Research Council Discovery Grant DP160101117 (to G.A.L., L.A.K., and A.G.C.) and National Health and Medical Research Council Early Career Researcher Fellowship 1111909 (to L.A.K.).

1. Susman RL (1983) Evolution of the human foot: Evidence from Plio-Pleistocene hominids. *Foot Ankle* 3:365–376.
2. Elftman H, Manter J (1935) The evolution of the human foot, with especial reference to the joints. *J Anat* 70:56–67.
3. Holowka NB, Lieberman DE (2018) Rethinking the evolution of the human foot: Insights from experimental research. *J Exp Biol* 221:jeb174425.
4. Lovejoy CO, Latimer B, Suwa G, Asfaw B, White TD (2009) Combining prehension and propulsion: The foot of Ardipithecus ramidus. *Science* 326:72e1–72e8.
5. Day MH, Napier JR (1964) Hominid fossils from Bed I, Olduvai Gorge, Tanganyika: Fossil foot bones. *Nature* 201:969–970.
6. Pontzer H, et al. (2010) Locomotor anatomy and biomechanics of the Dmanisi hominins. *J Hum Evol* 58:492–504.
7. Bojsen-Møller F (1979) Calcaneocuboid joint and stability of the longitudinal arch of the foot at high and low gear push off. *J Anat* 129:165–176.
8. Ker RF, Bennett MB, Bibby SR, Kester RC, Alexander RM (1987) The spring in the arch of the human foot. *Nature* 325:147–149.
9. Hicks JH (1954) The mechanics of the foot. II. The plantar aponeurosis and the arch. *J Anat* 88:25–30.
10. Mann R, Inman VT (1964) Phasic activity of intrinsic muscles of the foot. *J Bone Joint Surg Am* 46:469–481.
11. Kelly LA, Cresswell AG, Racinais S, Whiteley R, Lichtwark G (2014) Intrinsic foot muscles have the capacity to control deformation of the longitudinal arch. *J R Soc Interface* 11:20131188.
12. Kelly LA, Kuitunen S, Racinais S, Cresswell AG (2012) Recruitment of the plantar intrinsic foot muscles with increasing postural demand. *Clin Biomech (Bristol, Avon)* 27:46–51.
13. Kelly LA, Lichtwark G, Cresswell AG (2015) Active regulation of longitudinal arch compression and recoil during walking and running. *J R Soc Interface* 12:20141076.
14. Fiolkowski P, Brunt D, Bishop M, Woo R, Horodyski M (2003) Intrinsic pedal musculature support of the medial longitudinal arch: An electromyography study. *J Foot Ankle Surg* 42:327–333.
15. Kelly LA, Farris DJ, Lichtwark GA, Cresswell AG (2018) The influence of foot-strike technique on the neuromechanical function of the foot. *Med Sci Sports Exerc* 50:98–108.
16. Holowka NB, Wallace IJ, Lieberman DE (2018) Foot strength and stiffness are related to footwear use in a comparison of minimally- vs. conventionally-shod populations. *Sci Rep* 8:3679.
17. Kuo AD, Donelan JM, Ruina A (2005) Energetic consequences of walking like an inverted pendulum: Step-to-step transitions. *Exerc Sport Sci Rev* 33:88–97.
18. Kura H, Luo ZP, Kitaoka HB, An KN (1997) Quantitative analysis of the intrinsic muscles of the foot. *Anat Rec* 249:143–151.
19. Powell PL, Roy RR, Kanim P, Bello MA, Edgerton VR (1984) Predictability of skeletal muscle tension from architectural determinations in guinea pig hindlimbs. *J Appl Physiol* 57:1715–1721.
20. Fukunaga T, Roy RR, Shellock FG, Hodgson JA, Edgerton VR (1996) Specific tension of human plantar flexors and dorsiflexors. *J Appl Physiol (1985)* 80:158–165.
21. Spector SA, Gardiner PF, Zernicke RF, Roy RR, Edgerton VR (1980) Muscle architecture and force-velocity characteristics of cat soleus and medial gastrocnemius: Implications for motor control. *J Neurophysiol* 44:951–960.
22. Rao UB, Joseph B (1992) The influence of footwear on the prevalence of flat foot. A survey of 2300 children. *J Bone Joint Surg Br* 74:525–527.
23. Largey A, et al. (2007) Three-dimensional analysis of the intrinsic anatomy of the metatarsal bones. *J Foot Ankle Surg* 46:434–441.
24. Bojsen-Møller F, Lamoreux L (1979) Significance of free-dorsiflexion of the toes in walking. *Acta Orthop Scand* 50:471–479.
25. Honert EC, Bastas G, Zelik KE (2018) Effect of toe joint stiffness and toe shape on walking biomechanics. *Bioinspir Biomim* 13:066007.
26. Donelan JM, Kram R, Kuo AD (2002) Mechanical work for step-to-step transitions is a major determinant of the metabolic cost of human walking. *J Exp Biol* 205:3717–3727.
27. Takahashi KZ, Gross MT, van Werkhoven H, Piazza SJ, Sawicki GS (2016) Adding stiffness to the foot modulates soleus force-velocity behaviour during human walking. *Sci Rep* 6:29870.
28. Takahashi KZ, Worster K, Bruening DA (2017) Energy neutral: The human foot and ankle subsections combine to produce near zero net mechanical work during walking. *Sci Rep* 7:15404.
29. Zelik KE, Honert EC (2018) Ankle and foot power in gait analysis: Implications for science, technology and clinical assessment. *J Biomech* 75:1–12.
30. McDonald KA, et al. (2016) The role of arch compression and metatarsophalangeal joint dynamics in modulating plantar fascia strain in running. *PLoS One* 11:e0152602.
31. Hogberg P (1952) How do stride length and stride frequency influence the energy-output during running? *Arbeitsphysiologie* 14:437–441.
32. Cavanagh PR, Williams KR (1982) The effect of stride length variation on oxygen uptake during distance running. *Med Sci Sports Exerc* 14:30–35.
33. Umberger BR, Martin PE (2007) Mechanical power and efficiency of level walking with different stride rates. *J Exp Biol* 210:3255–3265.
34. Farris DJ, Sawicki GS (2012) The mechanics and energetics of human walking and running: A joint level perspective. *J R Soc Interface* 9:110–118.
35. Sawicki GS, Lewis CL, Ferris DP (2009) It pays to have a spring in your step. *Exerc Sport Sci Rev* 37:130–138.
36. Snyder KL, Farley CT (2011) Energetically optimal stride frequency in running: The effects of incline and decline. *J Exp Biol* 214:2089–2095.
37. Thompson MA, Hoffman KM (2017) Superficial plantar cutaneous sensation does not trigger barefoot running adaptations. *Gait Posture* 57:305–309.
38. Eils E, et al. (2002) Modified pressure distribution patterns in walking following reduction of plantar sensation. *J Biomech* 35:1307–1313.
39. Hoch MC, Russell DM (2016) Plantar cooling does not affect standing balance: A systematic review and meta-analysis. *Gait Posture* 43:1–8.
40. Azizi E, Brainerd EL, Roberts TJ (2008) Variable gearing in pennate muscles. *Proc Natl Acad Sci USA* 105:1745–1750.
41. Brockway JM (1987) Derivation of formulae used to calculate energy expenditure in man. *Hum Nutr Clin Nutr* 41:463–471.
42. Leardini A, et al. (2007) A new anatomically based protocol for gait analysis in children. *Gait Posture* 26:560–571.
43. Leardini A, et al. (2007) Rear-foot, mid-foot and fore-foot motion during the stance phase of gait. *Gait Posture* 25:453–462.
44. Farris D, Lichtwark G, Kelly L, Cresswell A (2019) Human foot muscle function during walking and running. The University of Queensland eSpace. Available at https://doi.org/10.14264/uql.2019.3. Deposited January 10, 2019.